Influence of nonstoichiometry on the Verwey transition

Ricardo Aragón and Douglas J. Buttrey
Department of Chemistry, Purdue University, West Lafayette, Indiana 47907

John P. Shepherd
Department of Physics, Purdue University, West Lafayette, Indiana 47907

Jurgen M. Honig
Department of Chemistry, Purdue University, West Lafayette, Indiana 47907
(Received 8 May 1984)

The dependence of the Verwey transition temperature on the nonstoichiometry of $Fe_{3(1-\delta)}O_4$ has been characterized by thermomagnetic analysis of the initial permeability in magnetite single crystals subjected to subsolidus controlled oxygen fugacity annealing. Nonstoichiometry depresses the transition temperature, which is a maximum for $\delta=0$. For extreme levels of cation deficiency, a second-order transition occurs at 120 K. An anomaly is reported at 250 K.

I. INTRODUCTION

The well known phase transition in magnetite, usually reported in the temperature range 115–124 K, has been the subject of numerous investigations since the early work by Verwey and Haajman.[1] Frequent reference has been made[2] to the influence of departures from ideal cation to oxygen stoichiometry in $Fe_{3(1-\delta)}O_4$ on the transition temperature. Recently,[3] calorimetric surveys of magnetite samples of varied origin have indicated that, in contrast to earlier reports,[4] a single, well defined first order peak can be found in carefully synthesized specimens. However, the characterization of nonstoichiometry over a comparatively narrow compositional range offers singular difficulties, which have promoted the use of indirect techniques, such as magnetic after-effects [cf. Ref. 3(b)]. The present study represents a first attempt at a systematic investigation of the influence of nonstoichiometry on the Verwey transition, in terms of independently verifiable phase equilibrium parameters, with special emphasis on sample preparation procedures.

II. NONSTOICHIOMETRY OF $Fe_{3(1-\delta)}O_4$

A. Equilibrium considerations

The description of nonstoichiometry in single phase magnetite and ferrite solid solutions in general, as a function of intrinsic oxygen fugacity (f_{O_2}) and temperature, is readily derived from the chemical equilibrium of the appropriate point defect model.[5] The fundamental aspects of this treatment are reviewed in this section.

It has been well established[6] that the point defect structure involves Frenkel disorder in the cation sublattice and that the ideal approximation is adequate for all but the highest departures from stoichiometry. Furthermore, allowance for the various possible point defect or cation site preference schemes does not substantially alter the magnitudes of the measurable equilibrium parameters of interest to this work.

In the Flood and Hill[7] convention, the Frenkel disorder reaction can be written as

$$\mathrm{Fe}\rightarrow V+I\ , \tag{1}$$

where V represents a vacancy and I an interstitial. The associated equilibrium constant, expressed in cation mole fractions for the ith species over the sum of cations and interstitials (n_i/n_Σ), is

$$K_1=n_V n_I/n_\Sigma^2\ , \tag{2}$$

since point-defect concentrations are small ($n_{\mathrm{Fe}}/n_\Sigma\simeq 1$). The creation of three fourths of a cation site by addition of an oxygen atom can be described by the oxidation reaction

$$\mathrm{Fe}^{2+}+\tfrac{1}{4}\mathrm{O}_2\rightarrow\mathrm{Fe}^{3+}+\tfrac{1}{2}\mathrm{O}^{2-}+\tfrac{3}{8}V\ , \tag{3}$$

or

$$\mathrm{Fe}^{2+}+\tfrac{1}{4}\mathrm{O}_2+\tfrac{3}{8}I\rightarrow\mathrm{Fe}^{3+}+\tfrac{1}{2}\mathrm{O}^{2-}\ , \tag{4}$$

and the respective equilibrium expressions,

$$K_2=\frac{n_{\mathrm{Fe}^{3+}}}{n_{\mathrm{Fe}^{2+}}}f_{\mathrm{O}_2}^{-1/4}\left[\frac{n_V}{n_\Sigma}\right]^{3/8} \tag{5}$$

and

$$K_3=\frac{n_{\mathrm{Fe}^{3+}}}{n_{\mathrm{Fe}^{2+}}}f_{\mathrm{O}_2}^{-1/4}\left[\frac{n_\Sigma}{n_I}\right]^{3/8}\ , \tag{6}$$

are linearly related by the Frenkel-disorder expression (2). The relation between equilibrium point-defect concentrations and the degree of nonstoichiometry is established, defining

$$\delta=(1/n_\Sigma)(n_V-n_I) \tag{7}$$

from mass-balance considerations. The electroneutrality constraint, derived from (3) or (4), is introduced as

$$n_V - n_I = \tfrac{1}{8}(n_{Fe^{3+}} - 2n_{Fe^{2+}}) . \quad (8)$$

From relations (2), (5), (7), and (8), it can be shown[7] that, for a magnetite phase of arbitrary stoichiometry, the intrinsic oxygen fugacity is related to the nonstoichiometry parameter by

$$f_{O_2}^{1/4} = \left[2 + \frac{24\delta}{1 - 8\delta - \delta/2 - (\delta^2/4 + K_1)^{1/2}}\right] \times \frac{1}{K_2}[\delta/2 + \tfrac{1}{2}(\delta^2 + 4K_1)^{1/2}]^{3/8} , \quad (9)$$

which reduces to

$$f^{*1/4}_{O_2} = 2\frac{K_1^{3/16}}{K_2} \quad (10)$$

for stoichiometric magnetite ($\delta = 0$).

In principle, the measurement of δ as a function of f_{O_2} and temperature suffices to evaluate K_2 and K_1. The most reliable data base for this purpose has been obtained by thermogravimetric titration at high temperature[8] (900—1400 °C), thereby avoiding the uncertainties associated with quenching procedures. With these results, the equilibrium parameters defined by (2) and (5) were found to be best represented here, as a function of absolute temperature (T), by

$$\log_{10} K_2 = \frac{4456\ \text{K}}{T} - 2.64 \quad (11)$$

and

$$\log_{10} K_1 = \frac{-10740\ \text{K}}{T} - 1.23 . \quad (12)$$

Departure from strict Arrhenius behavior has been reported for equilibrium parameters associated with the formation of interstitials[8] (i.e., equivalent to K_1 and K_3 in this notation). However, the influence of these terms becomes manifest close to the reduction boundary, where the data are sparse and affected by the highest experimental uncertainty. In any case, Eq. (12) provides a satisfactory approximation for the purposes of this work.

The logarithm of the intrinsic oxygen fugacity calculated with Eqs. (9)—(11) has been plotted as a function of inverse temperature in Fig. 1, for various values of the nonstoichiometry parameter δ, within the $Fe_{3(1-\delta)}O_4$-Fe_2O_3 and $Fe_{3(1-\delta)}O_4$-$Fe_{1-\xi}O$ boundaries.[9] $\log_{10} f_{O_2}$ for the stoichiometric phase ($\delta = 0$) plots as a straight line, as expected from (10)—(12), which is the asymptotic limit for two families of curves, corresponding to cation-deficient ($\delta > 0$) and cation-excess phases ($\delta < 0$). The concave ($\delta > 0$) and convex ($\delta < 0$) curvature, above and below the stoichiometric limit, respectively, results from the relative dominance of the enthalpy terms for the exothermic reaction (3) or the endothermic Frenkel disorder process (11).[10]

A representative isotherm for 1400 °C has been plotted in Fig. 2 to illustrate the sigmoidal dependence of δ as a function of $\log_{10} f_{O_2}$, which characterizes the thermogravimetric titration results reported in Ref. 5(e). It is apparent from these considerations that the investigation of

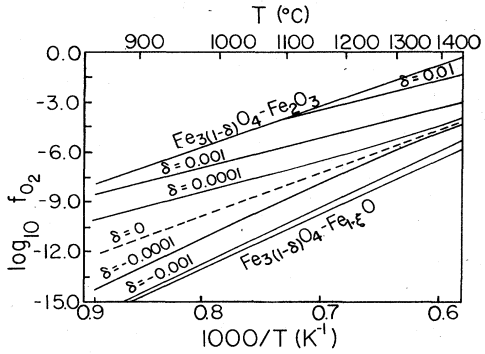

FIG. 1. Intrinsic oxygen fugacity for single-phase $Fe_{3(1-\delta)}O_4$, for various degrees of nonstoichiometry (δ) and stability field boundaries, as a function of inverse absolute temperature. The dashed line represents the stoichiometric limit.

the influence of nonstoichiometry requires subsolidus annealing, in f_{O_2} buffering[11] gas mixtures, with directly monitored[12] oxygen fugacity at the highest practical temperature, in order to achieve adequate levels of sample homogeneity over the widest possible nonstoichiometric range.

B. Kinetic considerations

The chemical reaction in a single-crystalline magnetite sample, which ensues during annealing, in response to the imposed oxygen fugacity, involves the loss or addition of oxygen at the surface of the crystal, followed by cation migration. The mass transport process is the rate-controlling stage. It can be shown[13] that the pertinent diffusion coefficient for this vacancy relaxation process is the "bulk" or "chemical" diffusion coefficient ($\tilde{D}$), which is proportional to the vacancy diffusion coefficient (D_V). The value of D_V may be derived from detailed experimental data[14] on the tracer-iron diffusion coefficient (D^*) as a function of oxygen fugacity and temperature, taking the ratio of D^* and the equilibrium vacancy concentration, with the result[15]

$$D_V = 0.143 \exp\left[\frac{-137\ \text{kJ/mol}}{RT}\right] , \quad (13)$$

in units of cm^2/sec. From the solution of Fick's second law for the boundary conditions of an infinite slab,[16] the

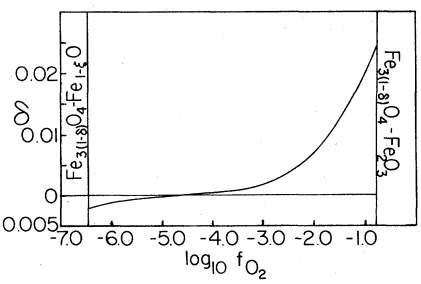

FIG. 2. Nonstoichiometry parameter δ as a function of $\log_{10} f_{O_2}$ at 1400 °C. The horizontal line represents the stoichiometric limit between cation-deficient ($\delta > 0$) and cation-excess ($\delta < 0$) phases.

parameter $D_V t/l^2$, where t is time and l is the half thickness of the slab, must be greater than 1.5 to ensure complete reaction. This procedure provides an estimate of the minimum annealing time, which should be increased to allow for uncertainties in D_V ($\simeq$30—50 %).

Similar considerations apply to the evaluation of the efficiency of the quenching procedure. The requirement to quench any given high temperature degree of nonstoichiometry can be satisfied only if the cooling time is insufficient for substantial reaction under the oxidizing conditions imposed by the gaseous buffer at lower temperatures. The rates calculated with Eq. (13) predict homogenization of a 0.5-mm-thick slab at 1400 °C in approximately 2 min. Therefore, it is impossible to avoid some measure of surface reaction on the sample during quenching. Instead, the size of the slabs should be optimized to allow for trimming of the inhomogeneous exterior, preserving a sizeable, useful sample.

III. THERMOMAGNETIC ANALYSIS

Substantial losses in the signal associated with the Verwey transition restrict the usefulness of electrical resistivity and calorimetry to monitor changes in the transition temperature (T_V) with increasing nonstoichiometry or doping. This limitation does not extend to the well established[17] discontinuous change in magnetocrystalline anisotropy energy.

Variations in magnetic anisotropy can be readily monitored through their influence on initial permeability (μ_i). In the limit of very low applied magnetic fields, for a demagnetized specimen, magnetic domain wall motion is entirely reversible and permeability is inversely proportional to the anisotropy energy.[18] Occasional use of μ_i thermal analysis (henceforth TMA) for Verwey-type transitions has been reported previously.[19] Relative measurements of μ_i have the advantage of requiring neither a particular state of aggregation of the sample nor provision for electrical contacts or mechanical displacement of the detector.

The instrumental requirements for this type of experiment are very modest. The basic design is a modified version of those in current use for ac determination of Curie points in ferromagnetic materials.[20] The technique involves placing the sample in the core of a transformer (1 cm o.d., 3 cm long, 20 turns) and using in-phase detection to recover the ac signal (10 kHz) induced in a secondary winding by coupling to the primary winding, which is driven by the internal oscillator of a lock-in amplifier (Princeton Applied Research model JB-6). The amplitude of the excitation signal to the primary winding is regulated by a current amplifier capable of a maximum 300-mA peak-to-peak output. A variable mutual inductance, wound in series opposition to the sample coils, provides for nulling of the signal coupling in the absence of a sample. The sample transformer is enclosed in a cryostat and the temperature is measured with a platinum-resistance thermometer (Omega RTD-TFD). The proportional output of the lock-in amplifier and the RTD resistance are processed in line by a computer (Hewlett-Packard model 85). The geometric parameters of the sample transformer, in conjunction with the limited applied currents ($\simeq$30 mA), ensure operation at very low fields ($\ll$1 Oe), under which the initial permeability regime is a reasonable assumption.

IV. EXPERIMENTAL DETAILS

The starting materials were magnetite single crystals grown by skull melting from 99.9%-pure Fe_2O_3 (Ref. 21), sliced into 3-mm-thick slabs. Annealing was carried out in a vertical furnace, at 1400 °C, 1200 °C, and 1000 °C, in appropriate CO_2-CO atmospheres,[11] regulated by precision Vacuum General 80-4 flowmeter controllers. Provision was made for direct f_{O_2} and temperature monitoring with an yttrium-stabilized zirconia electrolytic cell[22] with a sensitivity of 0.01 $\log_{10}$ atm units. The slabs were suspended in a Pt basket, either presaturated with iron at the same f_{O_2}-T conditions of the experiment, or weaved with 0.013-mm-thick wire for a minimal Pt-to-sample weight ratio ($\simeq 10^{-5}$), in order to avoid loss of Fe by alloying. Annealing times were conservatively set from 18 h at 1400 °C to 85 h at 1000 °C. For quenching purposes, the baskets were dropped into a water-cooled, jacketed cup. Finally, the surfaces of the slabs were removed by diamond-saw-sectioning, yielding centimeter-sized, tabular samples approximately 1-mm thick, which were verified to be single crystals by Laue backreflection x-ray diffraction.

V. RESULTS

The results of 60 representative experiments are summarized in this section.

A. Closely stoichiometric samples ($\delta \simeq 0$)

The broad features of a TMA experiment on a closely stoichiometric sample are shown in Fig. 3. Between room temperature and 130 K, μ_i is relatively insensitive to temperature. Polycrystalline samples and single crystals oriented with the hard magnetic axis [100] parallel to the search-coil axis tend to show more pronounced degrees of curvature, closely mirroring the temperature dependence of the cubic magnetic anisotropy constant.[17] Upon cooling, a maximum occurs between 128 and 130 K, followed by an almost linear signal attenuation, henceforth referred

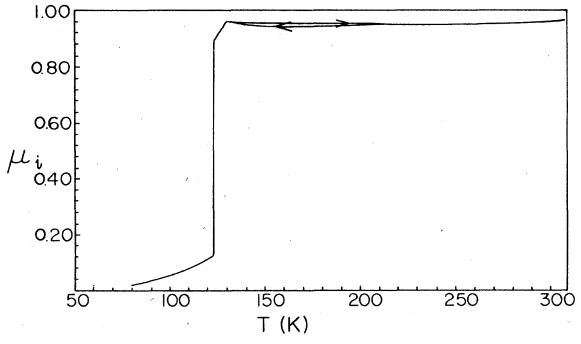

FIG. 3. Relative magnetic initial permeability (arbitrary scale) as a function of temperature for a magnetite single crystal annealed at $\log_{10} f_{O_2} = -5.0$ and 1400 °C for 19 h; $\delta = -0.000\,17$.

to as the "lead-in" to the transition. An abrupt drop in signal is observed at T_V, corresponding to the discontinuous increase in magnetic anisotropy. Below T_V, cooling induces a moderate further reduction in μ_i, in keeping with a gradual increase in anisotropy. The difference in temperature between the high and low ends of the discontinuity provides a measure of the width of the transition, which is typically <0.5 K for this type of sample. The barycenter for T_V ($122 < T_V < 125$ K) is taken at the midpoint between these extremes. Independent measurements of T_V on the same samples, by conventional four-probe dc-resistivity, Seebeck-coefficient, and calorimetric techniques (relaxation[23] and differential scanning calorimetry) agree within the accuracy of the RTD thermometry (0.25 K). Heating and cooling curves are identical and reproducible upon recycling. No appreciable thermal hysteresis is observed for T_V.

B. Moderately nonstoichiometric phases

Experiments on samples annealed between the reduction boundary and the stoichiometric limit show the same broad features described for closely stoichiometric specimens. For the highest levels of cation excess ($\delta=-0.001$), T_V is depressed to 120 K. Upon cooling, cation-deficient phases exhibit an increase in μ_i between 280 and 200 K (cf. Fig. 4). This temperature is poorly defined, because the change is gradual over 20—30 K and extremely irreversible; thermal hysteresis of 60—70 K is not uncommon (cf. Fig. 5), with a centroid at $\simeq$250 K. The magnitude of the change in μ_i increases with higher levels of cation deficiency; it is barely noticeable for $\delta\simeq0.001$ but equivalent to the discontinuity at T_V for $\delta\simeq0.01$. So far, corresponding anomalies have not been observed in dc-resistivity or heat-capacity experiments.

The μ_i maximum at 130 K is preserved for these compositions, but T_V is depressed proportionally to cation deficiency. The lowest recorded transition temperature observed so far is 82 K ($\delta=0.016$). The depression of T_V is accompanied by an increase in the width of the transition and, as revealed by preliminary relaxation-calorimetry investigations, a reduction in the transition entropy.

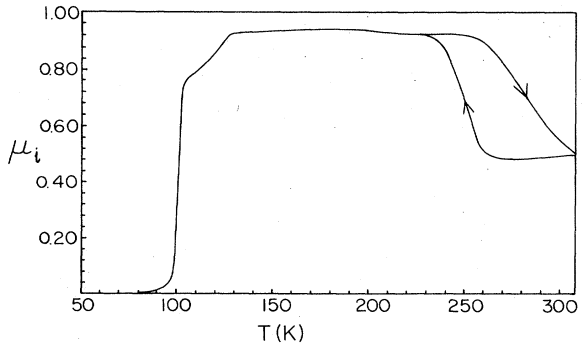

FIG. 4. Relative magnetic initial permeability (arbitrary scale) as a function of temperature for a magnetite single crystal annealed at $\log_{10} f_{O_2} = -2.0$ and 1400 °C for 18 h; $\delta=0.0068$.

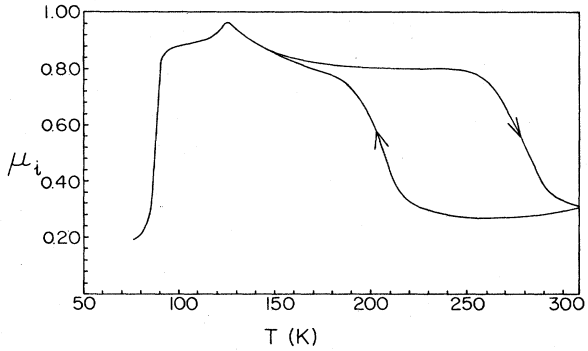

FIG. 5. Relative magnetic initial permeability (arbitrary scale) as a function of temperature for a magnetite single crystal annealed at $\log_{10} f_{O_2} = -1.5$ and 1400 °C for 20 h; $\delta=0.012$.

C. Highly cation-deficient phases

For extreme levels of cation deficiency ($\delta=0.02$), the sigmoidal signature in μ_i is found at 120 K (cf. Fig. 6), with a 5-K width. With the exception of a small degree of thermal hysteresis at the transition ($\simeq$1 K) and a moderate difference in the heating and cooling cycles above the critical temperature, these results are similar to those obtained for more stoichiometric phases. However, relaxation-calorimetry experiments offer conclusive evidence that, by contrast with the first order phenomenon normally observed at the Verwey temperature, this is a second order transition with no associated latent heat.

It was not possible to preserve a single phase in these samples, even with the use of liquid nitrogen or mercury rapid-quenching techniques. Microscopic examination revealed hematite segregation in association with partially inverted maghemite cation-deficient phases. Consequently, the value of δ is uncertain in these cases.

D. Oxidized and reduced phases

Since both $Fe_{1-\xi}O$ and Fe_2O_3 are weakly magnetic, there is no major restriction to the interpretation of TMA experiments on multiple-phase, oxidized $Fe_{3(1-\delta)}O_4$-Fe_2O_3 and reduced $Fe_{3(1-\delta)}O_4$-$Fe_{1-\xi}O$ mixtures. The signal from the magnetite component is dominant.

The results for reduced samples resemble those obtained for single-phase stoichiometric or cation-excess samples (cf. Fig. 7). A more pronounced degree of curvature is ob-

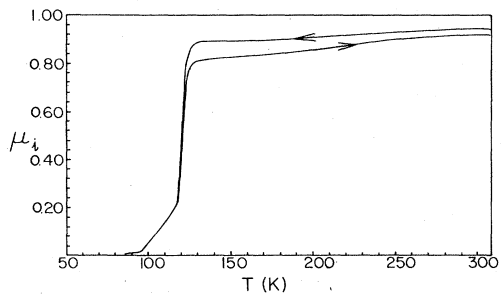

FIG. 6. Relative magnetic initial permeability (arbitrary scale) as a function of temperature for a magnetite single crystal annealed at $\log_{10} f_{O_2} = -1.0$ and 1400 °C for 13 h; $\delta=0.02$.

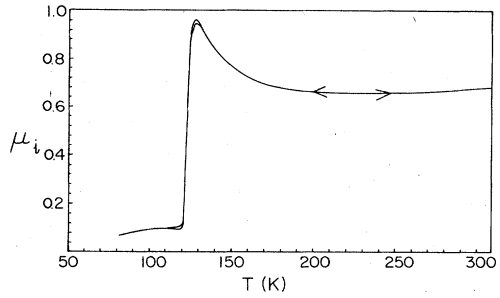

FIG. 7. Relative magnetic initial permeability (arbitrary scale) as a function of temperature for a reduced magnetite-wüstite intergrowth.

served above T_V (123 K) due to the polycrystalline nature of the material. There is no thermal hysteresis.

The basic features of cation-deficient phases can be recognized in the results for oxidized samples (cf. Fig. 8). The high-temperature inflection and its associated thermal lag are present but are subject to considerable broadening with temperature. The transition (T_V=96 K) is preceded by a large lead-in from the maximum, accounting for most of the total signal drop.

E. Isochemically annealed phases

It is apparent from the initial point defect considerations that a distinction must be made between point defect concentrations associated with nonstoichiometry which entail a change in the $[Fe^{3+}]/[Fe^{2+}]$ ratio [i.e., reactions (3) and (4)] and those changes derived from thermal Frenkel disorder [reaction (1)]. In order to test for the influence of Frenkel disorder on the Verwey transition, aliquots of closely stoichiometric samples prepared by CO_2-CO annealing at 1400 °C were encapsulated in sealed silica ampoules and reannealed at 1200 °C, 1000 °C, and 800 °C, which decreases the concentration of Frenkel pairs by up to 2 orders of magnitude [cf. Eq. (12)]. Within experimental uncertainty, the TMA results were indistinguishable from those obtained prior to isochemical annealing. Likewise, sealed-tube annealings, followed by slow furnace cooling (≃50 °C/h), designed to remove possible mechanical stress and avoid thermal shock during quenching, induced no further change in behavior.

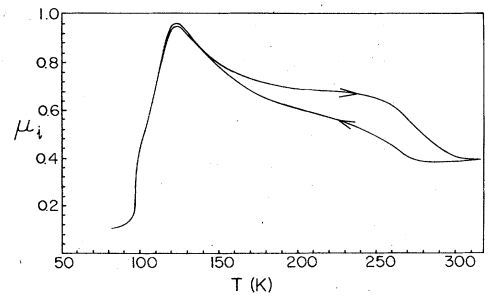

FIG. 8. Relative magnetic initial permeability (arbitrary scale) as a function of temperature for an oxidized magnetite-hematite intergrowth.

VI. DISCUSSION

The dependence of T_V on the annealing $\log_{10} f_{O_2}$ for the 1400 °C isotherm has been plotted in Fig. 9. The solid circle for each datum represents the inflection of the TMA curve, whereas the vertical bar is drawn between the temperatures for the extremes of the transition mode. The influence of the annealing f_{O_2} can be readily related to the titration curve for the nonstoichiometry parameter δ (cf. Fig. 2).

T_V seems relatively insensitive to f_{O_2} for the range $-6.4 < \log_{10} f_{O_2} < -4$, in which small departures from stoichiometry ($|\delta| < 0.001$) are induced. However, a drastic depression of T_V is apparent for more oxidizing atmospheres, concurrently with the steeply ascending branch of the titration curve (cf. Fig. 2).

Several factors contribute to the apparent increase in the width of the transition for progressively higher f_{O_2} conditions. The influence of the uncertainty in electrochemically monitored $\log_{10} f_{O_2}$ (0.01) is clearly a function of δ, which becomes substantial in this region ($\Delta\delta > 10^{-4}$). In addition, it is increasingly difficult to meet the quenching requirements because the oxygen chemical potential gradients increase by several orders of magnitude. For extreme degrees of nonstoichiometry (δ=0.02 and 0.016, dashed datum in Figs. 9 and 10), examination of the sample by reflected-polarized-light optical microscopy revealed areas with incipient formation of the "trellis" texture, characteristic of "oxi-exsolution" phenomena.[24] This fine intergrowth proved no obstacle to obtain Laue x-ray photographs, which were admitted as necessary rather than sufficient proof of homogeneity in this work.

It is apparent in Fig. 1 that slow cooling or sealed-tube reannealing of nonstoichiometric magnetite, at lower temperatures, leads to the crossing of the oxidation or the reduction boundaries, for cation-deficient or -excess phases, respectively.[25] This exsolution phenomenon is entirely isochemical, because the second phase, either Fe_2O_3 or $Fe_{1-\xi}O$, forms at the expense of the degree of nonstoichiometry. The remnant magnetite has a lower δ

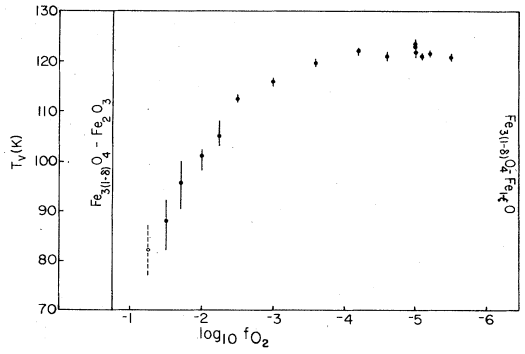

FIG. 9. Verwey transition temperature vs annealing $\log_{10} f_{O_2}$ at 1400 °C. T_V determined from the inflection of TMA curves (solid circles). Vertical bars indicate the width of the transition. Dashed datum represents a sample showing traces of oxidation.

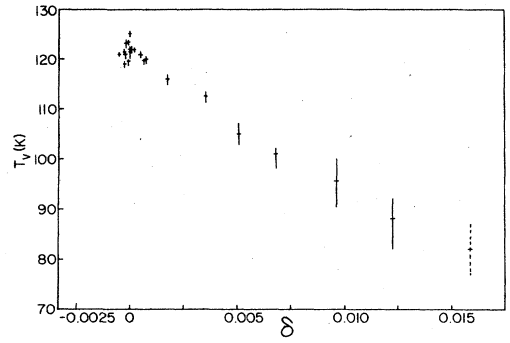

FIG. 10. Verwey transition temperature vs nonstoichiometry parameter δ for 28 samples annealed at 1400 °C, 1200 °C, and 1000 °C. Dashed datum represents a sample showing traces of oxidation.

value and, consequently, a higher T_V, than the parent phase.

Once a second phase is formed, the f_{O_2} is fixed by the binary equilibrium join. Under these conditions, cooling leads to the crossing of successive intrinsic f_{O_2} curves for lower $|\delta|$ values (cf. Fig. 1). The range of nonstoichiometry of magnetite in equilibrium with wüstite is relatively insensitive to temperature, as illustrated in Fig. 1 by the close parallelism of the $\delta=-0.001$ curve with the reduction boundary. The reduction assemblage contains a magnetite phase with a very narrow δ range, which yields a sharply defined TMA transition curve (cf. Fig. 7). However, the corresponding change in δ at the oxidation boundary for the same temperature range is almost 2 orders of magnitude. The wide range of associated T_V values induces the pronounced lead-in to the transition, evident in Fig. 8, for an oxidized sample.

In Fig. 10 the T_V values for 28 samples annealed at 1400 °C, 1200 °C, and 1000 °C have been plotted as a function of δ, calculated with Eqs. (9), (11), and (12). Within experimental error, the data fit the same general trend of lower T_V with departures from ideal stoichiometry. No attempt is made to approximate the dependence by any particular functional because this procedure would entail unwarranted implications for the nature of the transition.

For $|\delta| < 10^{-3}$ the scatter of the data exceeds the experimental uncertainty. At these low levels of nonstoichiometry, the chemical purity of the starting materials becomes competitive with δ in altering the $[Fe^{3+}]/[Fe^{2+}]$ ratio, which ultimately determines the value of T_V. Neutron activation analysis of representative samples revealed typical impurity concentrations of Na (10—200 ppm), Cr (50—100 ppm), Rb (25 ppm), and Co (5 ppm). The investigation of T_V in this δ range would require an improvement of 1—2 orders of magnitude in reagent purity. Work to this end is currently in progress.

By extension of the above arguments on the nature of the lead-in to the transition in TMA experiments, it is conceivable that, for very high purity stoichiometric Fe_3O_4, T_V may occur closer to the detected maximum for μ_i (130 K), which coincides with the temperature for minimum magnetic anisotropy and the onset of changes in Mössbauer spectra.[26]

In view of the strong dependence of T_V on δ and the difficulties in securing adequate sample homogeneity, the wide range of reported T_V values and the occurrence of "multiple" transitions[4] can be readily explained in terms of stoichiometric inhomogeneity. Recent calorimetric investigations[3] corroborate the existence of a single, well defined first order transition for carefully selected specimens. The depression of T_V with increasing nonstoichiometry is consistent with the influence of chemical dopants, in so far as both factors alter the $[Fe^{3+}]/[Fe^{2+}]$ ratio. It is not simple to reach an unambiguous conclusion with respect to the effects of stress, because thermal treatments designed to relieve strain may induce changes in composition, even in sealed-tube techniques, unless the starting material is very closely stoichiometric (cf. Fig. 1).

An additional new instance of the dramatic influence of nonstoichiometry is found in the change of order of the transition for extreme levels of cation deficiency. The pronounced decline of the transition temperature and entropy with δ is interrupted almost at the practical limit of quenching ($\delta=0.02$). Relaxation calorimetry indicates that a single, large ($\Delta C_p/C_p \simeq 2$) second order transformation appears at 120 K for this sample, without trace of any other anomaly between 4.2 and 300 K.

The origin of the μ_i inflection encountered at $\simeq$250 K for cation-deficient samples and its pronounced associated thermal hysteresis are unknown. Fe_2O_3 undergoes the well known Morin transition[27] at this temperature; however, the present samples are free of hematite, as verified by x-ray diffraction and polarized reflected light microscopy. Corresponding anomalies have not been observed in preliminary dc-resistivity and relaxation calorimetry experiments but a correlation has been found with discontinuities of up to 20 μV/K in the Seebeck coefficient. Additional, independent evidence for this phenomenon stems from an abrupt change in muon-spin-rotation frequency.[28]

VII. CONCLUSIONS

The results of this survey of the influence of nonstoichiometry on the Verwey transition are summarized here. Details of electrical transport and calorimetric measurements will be reported separately.

(1) The Verwey transition temperature is a maximum for pure, stoichiometric Fe_3O_4.

(2) Nonstoichiometry and chemical dopants depress T_V. Temperatures as low as 82 K have been detected; lower values may be possible with improved quenching techniques.

(3) For extreme degrees of nonstoichiometry, a second order transition is observed at 120 K.

(4) An anomaly in μ_i, affected by pronounced thermal hysteresis, occurs at $\simeq$250 K for cation-deficient phases.

ACKNOWLEDGMENTS

The authors are indebted to M. Yethiraj of the Missouri University Research Reactor for neutron activation analysis of the samples, to C. J. Sandberg and H. R. Har-

rison of the Purdue University Central Materials Preparation Facility and Q. W. Choi for their assistance with sample preparation, and to R. J. Rasmussen and J. W. Koenitzer for their supportive efforts in TMA and calorimetric measurements, respectively. One of us (R.A.) is thankful to G. Plenge for fruitful discussions on the application of TMA techniques, and to J. Snyder for assistance in early implementation of the hardware. This work was supported by the National Science Foundation under Grant No. DMR-81-03041-A02.

[1]E. J. Verwey and P. W. Haajman, Physica (Utrecht) **8**, 979 (1941); E. J. Verwey, P. W. Haajman, and F. C. Romeijn, J. Chem. Phys. **15**, 181 (1947).

[2]S. Iida, Philos. Mag. B **42**, 349 (1980); A. J. M. Kuipers and V. A. M. Brabers, Phys. Rev. B **20**, 594 (1979); H. P. Weber and S. S. Hafner, Z. Kristallogr. **133**, 327 (1971).

[3](a) J. P. Shepherd, J. W. Koenitzer, R. Aragón, C. J. Sandberg, and J. M. Honig (unpublished); (b) E. Gmelin, N. Lenge, and H. Kronmüller, Phys. Status Solidi A **79**, 465 (1983).

[4]J. J. Bartel and E. F. Westrum, Jr., J. Chem. Thermodyn. **8**, 583 (1976); J. J. Bartel, E. F. Westrum, Jr., and J. L. Haas, Jr., *ibid.* **8**, 575 (1976); M. O. Rigo, J. F. Mareche, and V. A. M. Brabers, Philos. Mag. B **48**, 421 (1983); B. J. Evans and E. F. Westrum, Jr., Phys. Rev. B **5**, 3791 (1972); J. J. Bartel and E. F. Westrum, Jr., in *Magnetism and Magnetic Materials—1972 (Denver),* proceedings of the 18th Annual Conference on Magnetism and Magnetic Materials, edited by C. D. Graham and J. J. Rhyne (AIP, New York, 1973), p. 1393; in *Magnetism and Magnetic Materials—1974 (San Francisco),* proceedings of the 20th Annual Conference on Magnetism and Magnetic Materials, edited by C. D. Graham, G. H. Lander, and J. J. Rhyne (AIP, New York, 1975), p. 86; M. O. Rigo, J. Kleinclauss, and A. J. Pointon, Solid State Commun. **28**, 1013 (1978); G. B. Falk, L. S. Pan, B. J. Evans, and E. F. Westrum, Jr., J. Chem. Thermodyn. **11**, 367 (1979); M. O. Rigo and J. Kleinclauss, Philos. Mag. B **42**, 393 (1980).

[5](a) H. Flood and D. G. Hill, Z. Elektrochem. **61**, 18 (1957); (b) R. Aragón and R. H. McCallister, Phys. Chem. Minerals **8**, 112 (1982); (c) R. Dieckmann and H. Schmalzried, Ber. Bunsenges. Phys. Chem. **81**, 344 (1977); (d) **81**, 414 (1977); (e) R. Dieckmann, *ibid.* **86**, 112 (1982).

[6]Compare Ref. 5(c).

[7]Compare Refs. 5(a) and 5(b).

[8]Compare Ref. 5(e).

[9]J. S. Huebner, in *Research Techniques for High Pressure and High Temperature,* edited by G. C. Ulmer (Springer, New York, 1971), pp. 123—179.

[10]Derived in Ref. 5(b).

[11]P. Deines, R. H. Nafziger, G. C. Ulmer, and E. Woermann, Bull. Earth Miner. Sci. Exp. Stn. Pa. State Univ. **88**, 32 (1974).

[12]R. J. Williams and O. Mullens, NASA Tech. Memo. X-58167 (1976).

[13]H. Schmalzried, *Solid State Reactions* (Academic, New York, 1974), p. 84.

[14]Compare Ref. 5(c).

[15]Compare Ref. 5(d).

[16]J. Crank, *The Mathematics of Diffusion* (Clarendon, Oxford, 1975).

[17]S. Chikazumi, in *Magnetism and Magnetic Materials—1975 (Philadelphia),* proceedings of the 21st Annual Conference on Magnetism and Magnetic Materials, edited by J. J. Becker, G. H. Lander, and J. J. Rhyne (AIP, New York, 1976), p. 382.

[18]H. Träuble, in *Magnetism and Metallurgy,* edited by A. E. Berkowitz and E. Kneller (Academic, New York, 1969), Vol. 2, p. 621.

[19]L. R. Bickford, Phys. Rev. **78**, 449 (1950); T. Merceron and J. L. Dormann, J. Magn. Magn. Mater. **15-18**, 1435 (1980).

[20]K. Strnat, G. Hoffer, and A. E. Ray, IEEE Trans. Magn. **MAG-3** 489 (1966).

[21]H. R. Harrison and R. Aragón, Mater. Res. Bull. **13**, 1097 (1978).

[22]J. P. Shepherd and C. J. Sandberg, Rev. Sci. Instrum. (to be published).

[23]Compare Ref. 3(a).

[24]S. E. Haggerty, in *Oxide Minerals,* Vol. 3 of *Short Course Notes,* edited by D. Rumble III (Mineralogical Society of America, Washington, D.C., 1976), pp. 1—100.

[25]Compare Ref. 5(b).

[26]J. L. Dormann, C. Djega-Mariadassou, and V. A. M. Brabers, in *Proceedings of the International Conference on the Applications of the Mössbauer Effect—1981 (Jaipur),* edited by V. G. Bhide (Indian National Science Academy, New Dehli, 1982), p. 196.

[27]F. J. Morin, Phys. Rev. **78**, 819 (1950).

[28]A. B. Denison, J. Appl. Phys. **55**, 2278 (1984).